ASTROBIOLOGY
Volume 6, Number 2, 2006


# Research Paper

# Impact Craters as Biospheric Microenvironments, Lawn Hill Structure, Northern Australia

JOHN LINDSAY[1] and MARTIN BRASIER[2]

## ABSTRACT

**Impact craters on Mars act as traps for eolian sediment and in the past may have provided suitable microenvironments that could have supported and preserved a stressed biosphere. If this is so, terrestrial impact structures such as the 18-km-diameter Lawn Hill Structure, in northern Australia, may prove useful as martian analogs. We sampled outcrop and drill core from the carbonate fill of the Lawn Hill Structure and recorded its gamma-log signature. Facies data along with whole rock geochemistry and stable isotope signatures show that the crater fill is an outlier of the Georgina Basin and was formed by impact at, or shortly before, approximately 509–506 million years ago. Subsequently, it was rapidly engulfed by the Middle Cambrian marine transgression, which filled it with shallow marine carbonates and evaporites. The crater formed a protected but restricted microenvironment in which sediments four times the thickness of the nearby basinal succession accumulated. Similar structures, common on the martian surface, may well have acted as biospheric refuges as the planet's water resources declined. Low-pH aqueous environments on Earth similar to those on Mars, while extreme, support diverse ecologies. The architecture of the eolian crater fill would have been defined by long-term ground water cycles resulting from intermittent precipitation in an extremely arid climate. Nutrient recycling, critical to a closed lacustrine sub-ice biosphere, could be provided by eolian transport onto the frozen water surface. Key Words: Martian analog—Impact craters—Cambrian—Lawn Hill Structure, northern Australia.** Astrobiology 6, 348–363.

## INTRODUCTION

THE SURFACE OF MARS is extensively cratered. Many of the craters show evidence of a sedimentary fill, the stratigraphy of which may ultimately provide a comprehensive record of the planet's later history (Fig. 1A). Perhaps more important, on a planet with limited and diminishing water resources, such craters may have provided a biospheric refuge or even a site for the evolution of a Late or post Noachian biosphere [$<$3.50 billion years ago (Ga)]. Craters with water ice ponded in them have recently been imaged on Mars (Fig. 1B) and may have been common in the past. If so, early terrestrial impact craters in suitable basinal settings may provide analogs for such environments.

[1]Lunar and Planetary Institute, Houston, Texas.
[2]Earth Sciences Department, Oxford University, Oxford, United Kingdom.

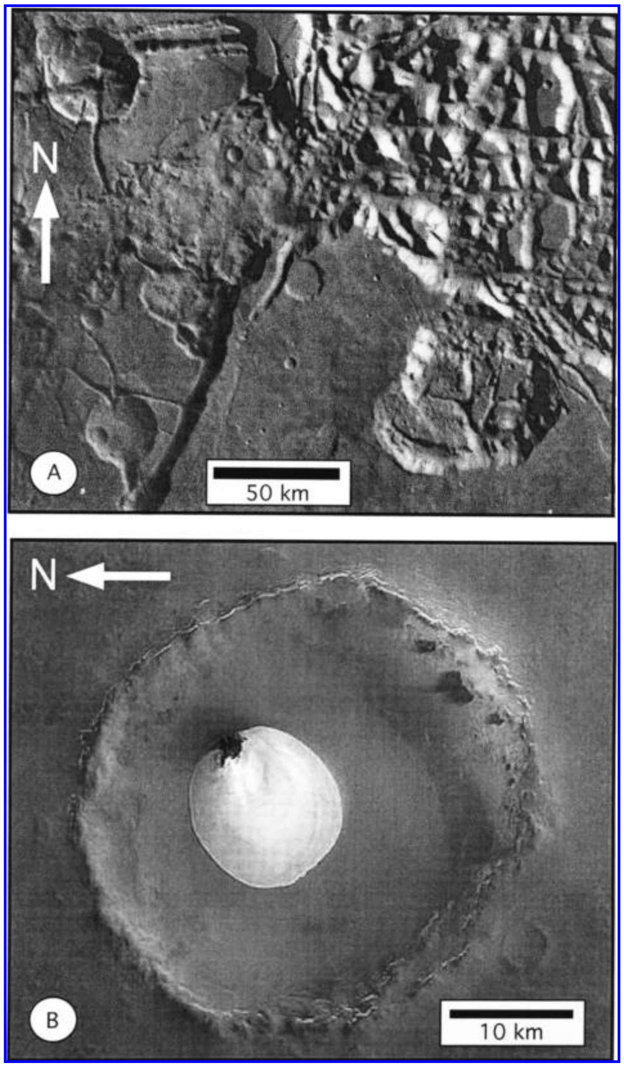


**FIG. 1.** **A:** Craters in southwest Hydraotes Chaos terrain region of Mars (00.50°S, 036.56°E). The craters are partially sediment filled and may contain a record of much of Mars' later history. Similar craters could have provided a biospheric refuge in the Late Noachian as the planet lost its hydrosphere (NASA image). **B:** A small crater 35 km in diameter and 2 km deep on the Vastitas Borealis area of Mars (70.5°N, 103.0°E). A significant volume of water ice remains trapped on the crater floor (ESA image).

The Earth has a very limited record of early impacts because its surface is constantly renewed as it is recycled by plate tectonics and refurbished by erosional processes. The record of a significant number of early impacts is, however, preserved on the more stable cratons. The Australian Craton, which is one of the most stable of Earth's crustal blocks, in particular, records a number of early impact events (Shoemaker and Shoemaker, 1996). One of these early structures, the Lawn Hill Structure in northern Australia (Figs. 2 and 3), contains a significant fill that may provide a useful martian analog. The carbonate rocks that form the crater fill at Lawn Hill have been tentatively correlated with the Middle Cambrian Thorntonia Limestone (Fig. 4) in nearby Georgina Basin, that is, the infilling of the Lawn Hill Structure may be an erosional outlier of the Georgina Basin. In this paper, we review the evidence for the age of the Lawn Hill Structure and evaluate stable carbon and oxygen isotope data from the sedimentary fill within the structure and from the nearby Georgina Basin in an attempt to determine the timing of the impact and its relationship to the basin. Finally, we assess the depositional facies preserved in the structure and evaluate the microenvironment within the crater as potential Mars analogs.

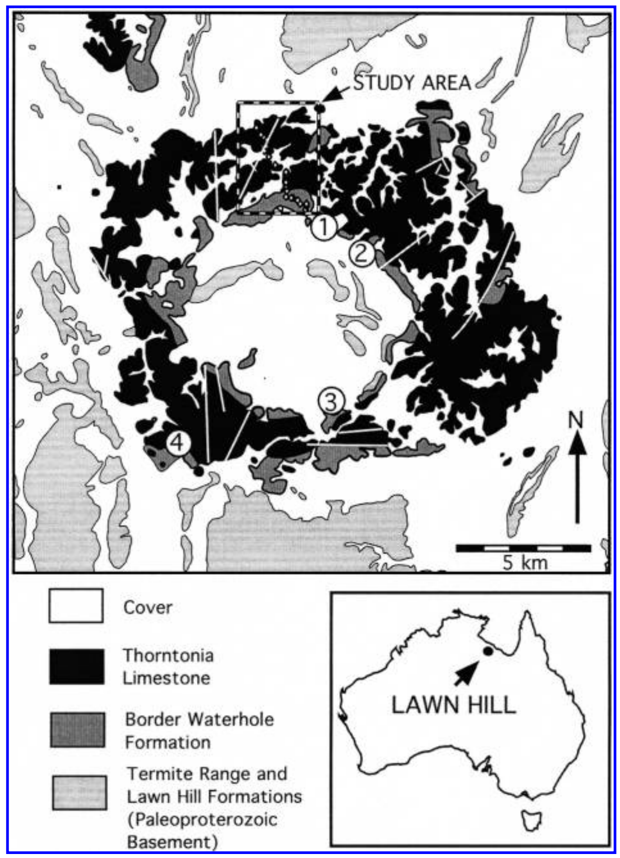


**FIG. 2. Simplified geological map of the Lawn Hill Structure showing the distinctive carbonate ring.** The main section sampled across the northern margin of the structure is outlined (see Fig. 3). Samples were also collected from basal silicified breccias at sites 1–3 and from drillcores LH116 and LH117 located at site 4. **Inset:** Map shows the location of the structure.

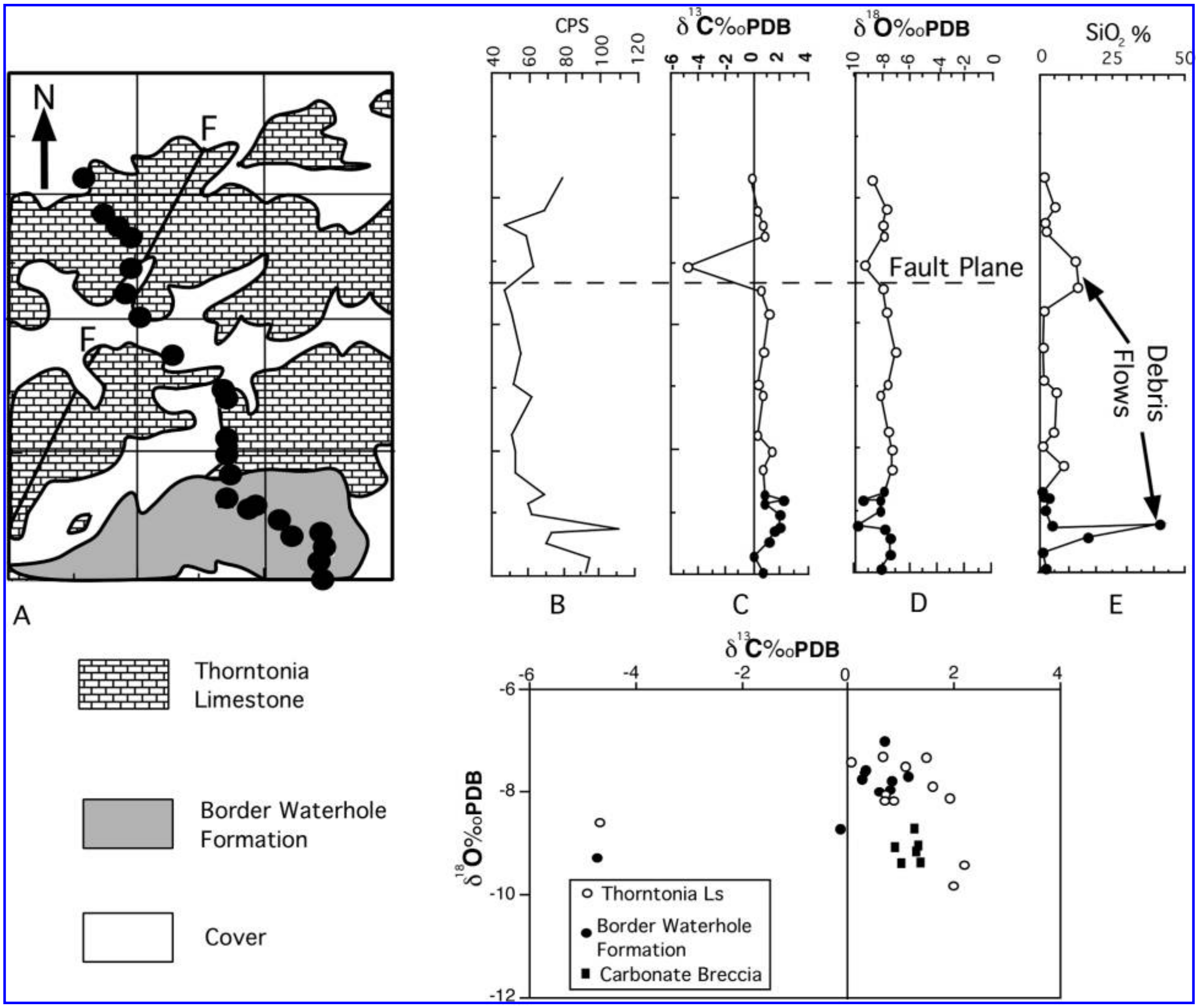


**FIG. 3.** **A:** Detailed map of the northern margin of the Lawn Hill carbonate ring structure showing sampling locations. **B:** Gamma log of the sampled section. CPS, counts/s. **C** and **D:** Carbon and oxygen isotope profiles. **E:** Silica content indicating the presence of clastic materials derived from debris flows. Panels B–E are projected onto a north–south profile along the section marked on the adjacent map. A 1-km UTM grid is shown. Ls, limestone. For location see Fig. 2.

## GEOLOGIC SETTING

### *The Georgina Basin*

The Neoproterozoic to Early Paleozoic Georgina Basin, which extends across much of north-central Australia, covering an area of approximately 325,000 km2, onlaps the southern margin of the Paleoproterozoic Mount Isa Basin to within 10 km of the Lawn Hill Structure. The main depocenter of the Georgina Basin lies considerably further south, such that the only formation associated with the basin exposed in the Lawn Hill area is the Middle Cambrian Thorntonia Limestone.

The Thorntonia Limestone, a platformal carbonate unit that seldom exceeds 100 m in thickness (Fig. 5), is sheet-like and widespread. It consists of dark gray dolomudstone and dolowackestone with occasional packstone and grainstone intervals. Fragmentary invertebrate bioclasts are abundant. Chert nodules and other textural indications of evaporite dissolution are present at well-defined levels (Southgate, 1988). Phosphatic hardgrounds are also present at a well-defined level within the formation. The Thorntonia Limestone forms a single depositional sequence that was deposited in a shallow, peritidal to subtidal setting during a major transgression that spanned the Ordian and early

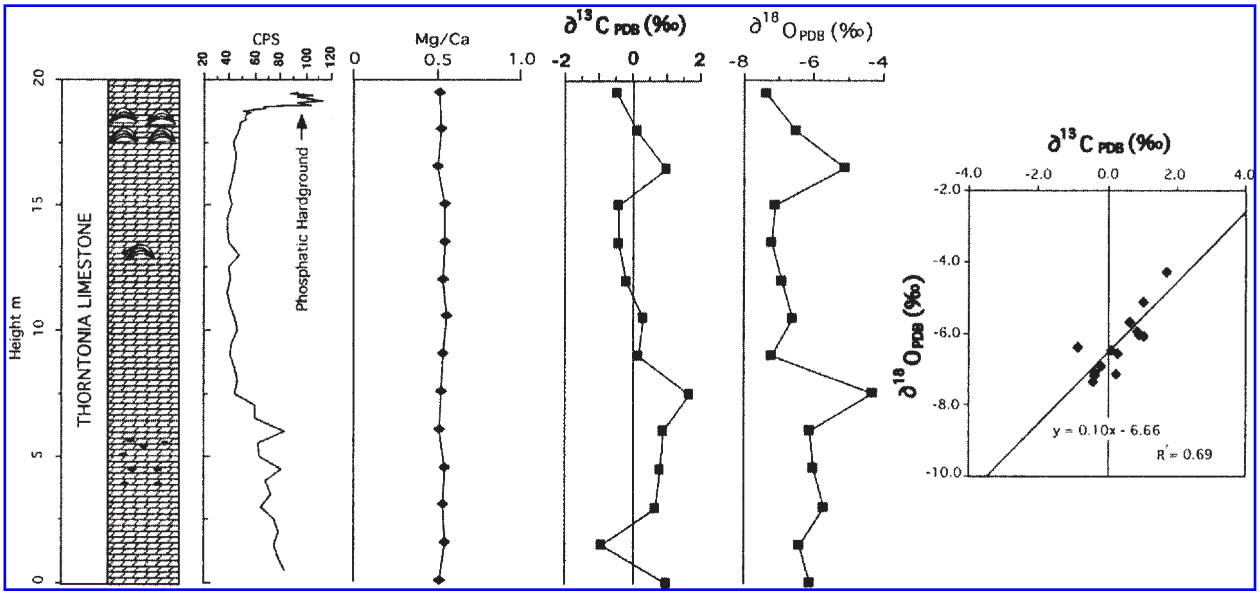


**FIG. 4. Reference section with gamma log through the lower Thorntonia Limestone on the O'Shannassy River 9 km to the south of Riversleigh Homestead (UTM Zone 54K, 0263751, 7884580).** Note the gamma-ray peak associated with the phosphatic hardground marking the maximum flooding surface. CPS, counts/s.

Templetonian [early Middle Cambrian, 509–506 million years ago (Ma)] (Ambrose *et al.*, 2001). Deposition occurred as a response to a basinal sag phase that resulted from the break up of Rodinia beginning in the Early Cambrian (for further discussion see Lindsay *et al.*, 1987; Lindsay and Korsch, 1989; Lindsay and Leven, 1996). The formation is thus a single depositional sequence deposited during a single sea-level cycle. The phosphatic hardgrounds represent the maximum flooding surface, the point at which water depth reached a maximum and when depositional rates were minimal. A lateral equivalent of this formation is believed to be the main lithology infilling the Lawn Hill Structure.

### *The Lawn Hill Structure*

The Lawn Hill Structure, a prominent 18-km-diameter carbonate ring structure, lies 250 km north of the town of Mount Isa at 18°40′S and 138°39′E (Fig. 2). The structure was first mapped by Öpik (1956) and Carter and Öpik (1961), and the carbonate rocks that form the ring tentatively correlated with the Thorntonia Limestone. For some time following its discovery the distinctive circular form of the structure led to speculation about its origin. De Keyser (1969) suggested that it was simply the product of local structural complexity. Wilson and Hutton (1980), after searching for evidence of impact or explosion, suggested that it may have been the product of solution collapse or collapse of a carbonate platform. Much later Hutton (1992) suggested an explosive volcanic origin for the structure. The Lawn Hill Structure was first identified as an impact structure by Stewart and Mitchell (1987), and their conclusions were confirmed by the later work of Shoemaker and Shoemaker (1996). As discussed below, the evidence for a hypervelocity impact origin for the Lawn Hill Structure is compelling.

The Lawn Hill Structure consists of three components: (1) the basement rocks in which the crater formed; (2) a massive breccia unit, the Border Waterhole Formation, which comprises the crater fill; and (3) the prominent carbonate ring structure that has been tentatively correlated with the Thorntonia Limestone in the Georgina Basin to the south.

*The basement*. The Lawn Hill Structure rests unconformably on the Paleoproterozoic rocks of the McNamara Group. Two formations, the Termite Range and Lawn Hill Formations, are exposed in the area (Fig. 2). The Lawn Hill Formation underlies most of the ring structure, while the Termite Range Formation is exposed on the southwestern margin of the structure. The Termite Range Formation, which is up to 950 m thick, con-

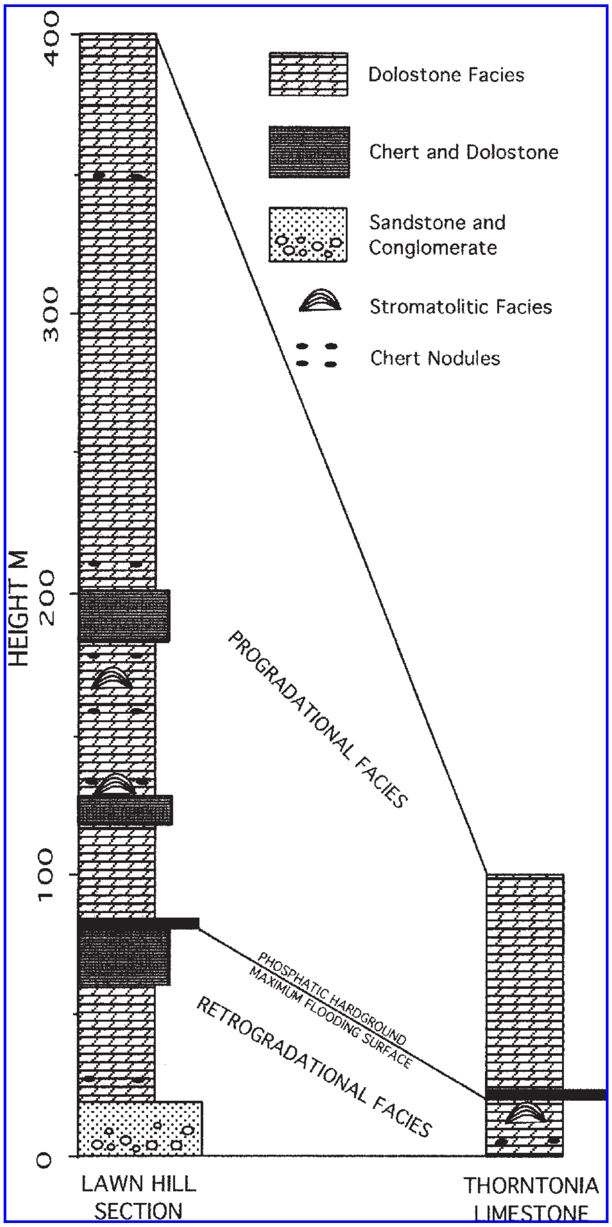


**FIG. 5. Composite stratigraphic section through the carbonate fill of the Lawn Hill Structure compared with a section through the Thorntonia Limestone in the nearby Georgina Basin.**

sists of interbedded coarse- to fine-grained lithic sandstone, graywacke, and siltstone units that form at least two broadly fining upward cycles deposited in a deep-water turbidite setting (Sweet and Hutton, 1982; Andrews, 1998). U-Pb SHRIMP zircon dating of the formation indicates a depositional age of approximately 1.63 Ga (Page *et al.*, 2000). The Lawn Hill Formation, which is 2,300 m thick and formed the main target for the impactor, consists of siltstones and fine-grained sandstone with tuffaceous intervals at a number of levels. U-Pb dating of tuffaceous intervals indicates depositional ages of from 1.616 to 1.595 Ga (Page *et al.*, 2000).

The rocks of the McNamara Group are poorly exposed in the area surrounding and within the Lawn Hill Structure. Despite the poor exposure, significant outcrops appear in the central area of the ring structure. Angular fragments of fine-grained sandstone and siltstone from the basal part of the Lawn Hill Formation are widely scattered and locally exhibit shatter cones. In the central area, suevites are present, which indicates partial melting of the fine-grained sediment produced the ropy textured lithology. The features were well documented by Stewart and Mitchell (1987) and further discussed by Shoemaker and Shoemaker (1996). Thin section analysis of the shatter cones shows that the quartz grains exhibit as many as three sets of closely spaced planar lamellae. Overall, these textural features leave little doubt that the central area of the Lawn Hill Structure is the central uplift of an impact generated crater that has been raised to shock pressures of approximately 12 GPa (Stewart and Mitchell, 1987).

*The basal breccias*. The Border Waterhole Formation, which consists of a massive poorly sorted breccia of angular chert clasts, is exposed, for the most part, as a discontinuous ring inside the main carbonate structure. In addition, small outcrops of the formation are present outside the ring structure on the northeastern and southern side of the crater (Figs. 2 and 3). The breccias interfinger laterally with the gray limestones and dolostones of the main carbonate ring. Where the unit is close to the basement contact, it contains a small proportion of rounded clasts that are possibly derived from the basement. The breccia is cemented, for the most part, by silica but locally may be cemented by fine-grained carbonate.

The contact between the Border Waterhole Formation and the central zone of the crater was studied in considerable detail. The contact is sharp and consistent over large distances. Directly beneath the contact we located siliceous breccias with a distinctive texture, which appear to predate the Border Waterhole Formation. Clasts, which are all quartz or at least siliceous, have a large grainsize range and, more importantly, have considerable range in their degree of roundness (Fig. 6A). For the most part, the brec-

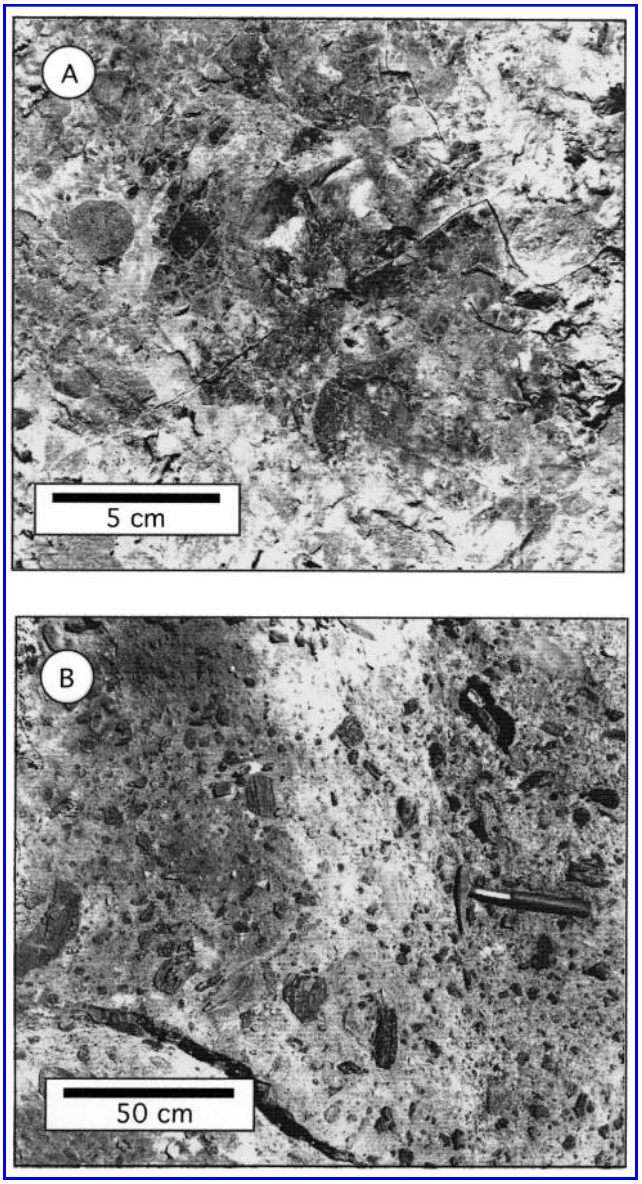


**FIG. 6. Breccias from (A) the base of the crater fill showing the predominance of silica clasts and (B) a polymict breccia from within the carbonate fill.**

cia is silica-cemented, though carbonate cement was encountered. These breccias are very different texturally from those encountered either in the Border Waterhole Formation or the breccia dikes (discussed below).

*The carbonate ring structure*. The main ring structure, which is exposed as a series of distinctive low karstic hills of gray limestone and dolostone, is a complex sedimentary body. The outcrops superficially appear chaotic because they are exposed as a series of blocks with an apparent complex bedding pattern, which suggests major structural deformation. However, when studied in detail the stratigraphy has considerable lateral continuity. Szulc (1992) found similar relationships on the southwestern side of the structure and was able to develop a simplified and idealized stratigraphy for the area. Using drill core and outcrop, we have been able to confirm that the fill is 200–400 m thick, considerably thicker than the Thorntonia Limestone to the south (Fig. 5). There are, however, many similarities to the Thorntonia Limestone in the preserved facies succession.

The dominant facies encountered in the carbonates of the Lawn Hill Structure are algal boundstones, a significant proportion of which have been dolomitized and recrystallized. Skeletal and peloidal grainstones are present in significant proportions toward the base and the top of the succession along with micritic intervals. The skeletal component is mostly derived from brachiopods, crinoids, hyoliths, and trilobites in a coarse, at times cross-bedded, coquina. Oncolites and oolites are present as thin units, especially in the middle of the formation. Chert nodules and other pseudomorphs indicative of evaporitic minerals (*cf*. Southgate, 1988) occur at a number of levels throughout the section.

Two other distinctive facies, a phosphatic hardground and a conglomeratic sandstone, occur in the middle and at the base of the succession, respectively, while a third facies, carbonate breccia dikes, project into the Paleoproterozoic basement rocks beneath the crater fill. All three facies are important in understanding the origins of the crater fill.

The basal conglomeratic sandstone, a 10–15-m unit, is largely medium-grained quartz with smaller proportions of less stable feldspar. Locally, pebble- to granule-sized clasts predominate. The unit rests unconformably on the Paleoproterozoic Lawn Hill Formation and fines upward from conglomeratic units at the base to finer sandstone at the top. The grains are bonded by a mixed hematitic and carbonate cement.

Beneath the ring structure, breccia dikes cross-cut the underlying Proterozoic basement rocks. The dikes are relatively common and were intersected in a number of drillcores where they were found to extend to depths in excess of 200 m (Andrews, 1991). Drill core records suggest that the dikes may completely surround some large blocks that are only slightly displaced (*cf*. Sturkell and Ormo, 1997).

The breccias consist of chert and limestone clasts set in a fine-grained matrix of carbonate. The matrix is generally relatively featureless and recrystallized. The relationship between the dikes and the transgressive basal sandstone and underlying siliceous breccia is not clear. They appear to be mutually exclusive with dikes occurring in the deeper parts of the crater, while the transgressive sandstone and siliceous breccia are confined to the inner margin of the ring and associated with the uplifted core of the structure. Transgressive sandstones have not been observed to be in contact with the dikes.

The phosphatic hardgrounds, which occur approximately 70 m above the base of the succession, consist of micritic lime muds and peloidal grainstones that are overlain by a distinctive burrowed phosphatic grainstone forming a well-defined surface. The phosphate replaces carbonate; in particular, invertebrate skeletal debris. Glauconite is also present locally.

A fragmentary fauna within the carbonates includes hyoliths, lingulid and orthid brachiopods, monoplacophorans, echinoderms, and polymerid trilobites. Szulc (1992) concluded that the fauna was typical of the Middle Cambrian but not distinctive enough to provide a more precise age.

## MATERIALS AND METHODS

To develop a comprehensive picture of the Lawn Hill Structure, three sites were sampled in preparation for geochemical analysis:

1. A reference section in the Thorntonia Limestone to the south of Riversleigh Homestead to allow a direct comparison of the Lawn Hill Structure carbonates with the carbonates of the Georgina Basin (Table 1 and Fig. 4).
2. A section across the northern side of the carbonate ring structure (Table 2 and Figs. 2 and 3).
3. Drillcores penetrating carbonate breccia and basement rocks beneath the ring structure to help determine the origin and timing of the emplacement of the dikes (Table 3).

### *Analytical method*

Natural gamma-ray signatures were measured at all outcrop sites using a handheld scintillometer. Readings were averaged over a 10-s period. Gamma-ray logging, a standard oil industry tool, provides data on the decay of radioactive elements, in particular U, Th, and K. For the most part these elements bond to clays, which allows a qualitative evaluation of shale (*i.e.*, clastic) content in the carbonate rocks. The technique has

TABLE 1. GEOCHEMISTRY OF SAMPLES COLLECTED FROM THE THORNTONIA LIMESTONE REFERENCE SECTION ON THE O'SHANNASSY RIVER, RIVERSLEIGH STATION, NORTHERN AUSTRALIA (FIG. 4)

| *Sample number* | *Height (m)* | *Whole rock geochemistry of carbonate* | | | | | | | | | | *Stable isotopes* | |
|---|---|---|---|---|---|---|---|---|---|---|---|---|---|
| | | *$SiO_2$* | *$Al_2O_3$* | *$Fe_2O_3$ (total)* | *MnO* | *MgO* | *CaO* | *$Na_2O$* | *$K_2O$* | *$P_2O_5$* | *Ni* | *$C_{carbonate}$* | *$O_{carbonate}$* |
| TT00 | 0.0 | 0.56 | 0.02 | 0.63 | 0.04 | 19.08 | 31.76 | 0.16 | 0.01 | 0.31 | 7 | 1.0 | −6.1 |
| TT01 | 1.5 | 1.51 | 0.00 | 0.09 | 0.03 | 19.76 | 30.73 | 0.15 | 0.01 | 0.26 | 2 | −0.9 | −6.4 |
| TT02 | 3.0 | 0.60 | 0.03 | 0.14 | 0.04 | 19.71 | 30.98 | 0.57 | 0.05 | 0.28 | 2 | 0.7 | −5.7 |
| TT03 | 4.5 | 0.40 | 0.00 | 0.16 | 0.05 | 19.48 | 30.45 | 0.17 | 0.02 | 0.38 | 3 | 0.8 | −6.0 |
| TT04 | 6.0 | 0.52 | 0.01 | 0.43 | 0.06 | 19.20 | 31.48 | 0.18 | 0.02 | 0.32 | 5 | 0.9 | −6.1 |
| TT05 | 7.5 | 0.37 | 0.00 | 0.07 | 0.06 | 19.39 | 31.59 | 0.37 | 0.02 | 0.08 | 2 | 1.7 | −4.3 |
| TT06A | 9.0 | 0.25 | 0.00 | 0.06 | 0.06 | 19.66 | 31.28 | 0.18 | 0.01 | 0.07 | 1 | 0.2 | −7.2 |
| TT06B | 10.5 | 0.60 | 0.00 | 0.08 | 0.08 | 20.10 | 30.81 | 0.14 | 0.00 | 0.13 | 3 | 0.3 | −6.6 |
| TT07 | 12.0 | 0.31 | 0.00 | 0.13 | 0.06 | 19.77 | 31.34 | 0.16 | 0.01 | 0.19 | 2 | −0.2 | −6.9 |
| TT08 | 13.5 | 0.45 | 0.00 | 0.14 | 0.06 | 19.71 | 30.81 | 0.14 | 0.01 | 0.27 | 2 | −0.4 | −7.2 |
| TT09 | 15.0 | 0.46 | 0.00 | 0.13 | 0.07 | 19.59 | 30.42 | 0.16 | 0.02 | 0.17 | 3 | −0.4 | −7.1 |
| TT10 | 16.5 | 1.02 | 0.10 | 0.12 | 0.07 | 18.19 | 30.99 | 0.45 | 0.09 | 0.38 | 3 | 1.0 | −5.1 |
| TT11 | 18.0 | 5.40 | 0.00 | 0.14 | 0.08 | 18.44 | 29.96 | 0.15 | 0.01 | 0.22 | 3 | 0.1 | −6.5 |
| TT12 | 19.5 | 2.71 | 0.00 | 0.17 | 0.04 | 18.78 | 31.01 | 0.15 | 0.01 | 1.22 | 3 | −0.4 | −7.4 |
| Mean | | 1.1 | 0.0 | 0.2 | 0.1 | 19.3 | 31.0 | 0.2 | 0.0 | 0.3 | 2.9 | 0.3 | −6.3 |
| SD | | 1.4 | 0.0 | 0.2 | 0.0 | 0.5 | 0.5 | 0.1 | 0.0 | 0.3 | 1.5 | 0.7 | 0.9 |

All oxides shown as percentages; Ni is in parts per million. Stable isotopes are shown as parts per million PDB. SD, standard deviation.

TABLE 2. GEOCHEMISTRY OF SAMPLES COLLECTED FROM A SECTION ACROSS THE NORTHERN MARGIN OF THE LAWN HILL STRUCTURE (FIG. 3)

| Sample number | Whole rock geochemistry | | | | | | | | | | Stable isotopes | | Location UTM Zone 54K | |
|---|---|---|---|---|---|---|---|---|---|---|---|---|---|---|
| | $SiO_2$ | $Al_2O_3$ | $Fe_2O_3$ (total) | MnO | MgO | CaO | $Na_2O$ | $K_2O$ | $P_2O_5$ | Ni | $C_{carbonate}$ | $O_{carbonate}$ | East | North |
| Carbonate | | | | | | | | | | | | | | |
| LH01 | 1.79 | 0.06 | 1.17 | 0.29 | 19.11 | 30.51 | 0.19 | 0.06 | 0.29 | 4 | 0.7 | −8.1 | 252444 | 7936023 |
| LH02 | 0.75 | 0.00 | 0.65 | 0.20 | 19.59 | 30.70 | 0.16 | 0.03 | 0.08 | 2 | 0.1 | −7.4 | 252408 | 7936146 |
| LH03 | 15.75 | 0.13 | 0.42 | 0.11 | 16.71 | 26.61 | 0.16 | 0.12 | 0.59 | 3 | 1.1 | −7.5 | 252458 | 7936267 |
| LH04 | 41.09 | 0.03 | 0.10 | 0.01 | 2.89 | 29.58 | 0.16 | 0.05 | 0.38 | 2 | 2.0 | −9.8 | 252429 | 7936372 |
| LH05 | 3.96 | 0.61 | 0.26 | 0.08 | 18.39 | 30.44 | 0.19 | 0.20 | 0.30 | 2 | 1.6 | −7.9 | 252200 | 7396342 |
| LH06 | 1.36 | 0.07 | 0.26 | 0.07 | 17.83 | 32.93 | 0.18 | 0.05 | 0.96 | 3 | 1.9 | −8.2 | 252104 | 7396480 |
| LH07 | 2.64 | 0.01 | 0.05 | 0.01 | 0.91 | 54.26 | 0.26 | 0.06 | 0.28 | 0 | 2.2 | −9.4 | 251931 | 7936590 |
| LH08 | 0.58 | 0.00 | 0.33 | 0.25 | 16.43 | 34.92 | 0.19 | 0.01 | 0.93 | 2 | 0.9 | −8.2 | 251875 | 7936581 |
| LH09 | 0.85 | 0.00 | 0.16 | 0.08 | 19.32 | 31.51 | 0.19 | 0.01 | 0.69 | 1 | 0.8 | −7.8 | 251686 | 7936638 |
| LH10 | 8.05 | 0.00 | 0.10 | 0.02 | 18.75 | 28.62 | 0.16 | 0.01 | 0.06 | 0 | 0.7 | −7.3 | 251706 | 7936832 |
| LH11 | 0.29 | 0.00 | 0.14 | 0.02 | 20.14 | 31.03 | 0.17 | 0.01 | 0.02 | 1 | 1.4 | −7.3 | 251693 | 7936991 |
| LH12 | 4.73 | 0.00 | 0.14 | 0.00 | 19.44 | 29.52 | 0.15 | 0.00 | 0.04 | 1 | 0.4 | −7.6 | 251697 | 7937122 |
| LH13 | 5.33 | 0.00 | 0.10 | 0.00 | 19.09 | 29.74 | 0.15 | 0.01 | 0.07 | 2 | 0.7 | −8.2 | 251698 | 7937428 |
| LH14 | 0.97 | 0.09 | 0.21 | 0.02 | 19.69 | 30.47 | 0.26 | 0.03 | 0.01 | 1 | 0.3 | −7.6 | 251675 | 7937521 |
| LH15 | 0.49 | 0.00 | 0.07 | 0.01 | 19.94 | 30.75 | 0.27 | 0.02 | 0.02 | 1 | 0.7 | −7.0 | 251276 | 7937775 |
| LH16 | 0.95 | 0.00 | 0.07 | 0.00 | 20.14 | 30.50 | 0.17 | 0.01 | 0.01 | 0 | 1.1 | −7.7 | 251034 | 7938083 |
| LH17 | 13.45 | 0.12 | 0.23 | 0.06 | 17.50 | 26.86 | 0.15 | 0.04 | 0.18 | 1 | 0.6 | −8.0 | 250886 | 7938268 |
| LH18 | 12.51 | 0.21 | 0.42 | 0.10 | 16.43 | 28.38 | 0.18 | 0.06 | 0.39 | 2 | −4.7 | −9.3 | 250958 | 7938461 |
| LH19 | 1.70 | 0.15 | 0.32 | 0.12 | 19.52 | 30.41 | 0.18 | 0.04 | 0.30 | 2 | 0.8 | −8.0 | 250947 | 7938703 |
| LH20 | 1.15 | 0.00 | 0.38 | 0.09 | 19.96 | 30.68 | 0.18 | 0.01 | 0.22 | 2 | 0.7 | −8.0 | 250842 | 7938788 |
| LH21 | 4.84 | 0.21 | 0.36 | 0.12 | 19.13 | 29.43 | 0.17 | 0.10 | 0.25 | 2 | 0.3 | −7.7 | 250749 | 7938908 |
| LH22 | 0.95 | 0.00 | 0.39 | 0.21 | 19.18 | 31.21 | 0.22 | 0.00 | 0.45 | 4 | −0.2 | −8.8 | 250582 | 7939159 |
| Mean | 5.65 | 0.08 | 0.29 | 0.09 | 17.28 | 31.32 | 0.19 | 0.04 | 0.30 | 1.73 | 0.64 | −8.04 | | |
| SD | 9.12 | 0.14 | 0.25 | 0.09 | 5.12 | 5.42 | 0.04 | 0.05 | 0.28 | 1.12 | 1.34 | 0.71 | | |
| Breccia | | | | | | | | | | | | | | |
| LH23 | 88.14 | 1.76 | 5.47 | 0.01 | 0.11 | 0.27 | 0.06 | 0.20 | 1.16 | 7 | | | 253107 | 7935635 |
| LH24 | 41.25 | 2.09 | 2.81 | 0.22 | 0.23 | 27.29 | 0.20 | 0.13 | 16.95 | 49 | −4.6 | −8.6 | 254520 | 7934617 |
| LH25 | 97.75 | 0.53 | 0.70 | 0.01 | 0.03 | 0.16 | 0.04 | 0.06 | 0.29 | 4 | | | 253414 | 7929048 |

All oxides shown as percentages; Ni is shown as parts per million. Stable isotopes are shown as parts per million PDB. SD, standard deviation.

been used on outcrop following the work of Chamberlain (1984).

Core samples and hand specimens of carbonate rocks collected in the field (see Tables 1–3) were examined macro- and microscopically for lithologic variation. Half of each sample was crushed for major and trace element whole rock geochemical analysis, and the remaining sample was retained for stable isotope and thin section analysis. Whole rock analyses of major and trace element geochemistry (see Tables 1–3) was carried out by x-ray resonance fluorescence and inductively coupled plasma mass spectrometry on all samples collected.

Stable isotope analysis was carried out in the laboratories of the Earth Sciences Department at Oxford University (Oxford, UK). Selected portions of carbonate were cleaned and analyzed using a VG Isomass (Cheshire, UK) PRISM mass spectrometer attached to an on-line VG Isocarb preparation system (*cf*. Brasier *et al*., 1996). Reproducibility of replicate standards was better than 0.1% for $\delta^{13}C_{carbonate}$ and $\delta^{18}O_{carbonate}$. Calibration to the Vienna Pee Dee Belemnite (PDB) standard via National Bureau of Standards 19 and Cambridge Carrara marble was performed daily using the Oxford in-house standard (NOCZ) (Brasier *et al*., 1994). Duplicate analyses were performed to evaluate isotopic variation among the various carbonate phases (up to six phases were analyzed). In general, the differences between phases were minimal and within analytical error. Duplicate $\delta^{13}C_{carbonate}$ analyses varied by between 0.01% and 0.30%, and $\delta^{18}O_{carbonate}$ values ranged between 0.5% and 0.9%. Overall the results show that the isotopic composition within samples is relatively uniform. Replicate analyses were also performed on all samples that exceed the mean

TABLE 3. GEOCHEMISTRY OF SAMPLES COLLECTED FROM CORES PENETRATING THE CARBONATE RING COMPLEX OF THE LAWN HILL STRUCTURE

| *Drillcore, sample number* | *Depth (m)* | *Whole rock geochemistry* | | | | | | | | | | *Stable isotopes* | |
|---|---|---|---|---|---|---|---|---|---|---|---|---|---|
| | | $SiO_2$ | $Al_2O_3$ | $Fe_2O_3$ (total) | *MnO* | *MgO* | *CaO* | $Na_2O$ | $K_2O$ | $P_2O_5$ | *Ni* | $C_{carbonate}$ | $O_{carbonate}$ |
| LH116 | | | | | | | | | | | | | |
| LH116-212.8 | 212.8 | 3.45 | 0.09 | 4.19 | 1.03 | 16.26 | 29.06 | 0.20 | 0.08 | 0.01 | 5 | 1.3 | −9.0 |
| LH116-214.2 | 214.2 | 67.74 | 6.78 | 2.72 | 0.02 | 0.58 | 0.67 | 0.72 | 1.71 | 0.38 | 13 | | |
| LH116-214.3 | 214.3 | 2.10 | 0.07 | 4.46 | 1.14 | 16.19 | 29.75 | 0.18 | 0.07 | 0.02 | 5 | 1.3 | −9.1 |
| LH117 | | | | | | | | | | | | | |
| LH117-154.3 | 154.3 | 3.79 | 0.12 | 2.58 | 0.62 | 17.43 | 29.23 | 0.25 | 0.11 | 0.22 | 3 | | |
| LH117-162 | 162.0 | 3.18 | 0.16 | 3.36 | 0.75 | 17.21 | 29.34 | 0.18 | 0.12 | 0.06 | 3 | 1.0 | −9.3 |
| LH117-165.4 | 165.4 | 71.19 | 3.95 | 7.41 | 0.12 | 1.64 | 2.90 | 0.05 | 1.13 | 0.30 | 21 | | |
| LH117-170.5 | 170.5 | 40.08 | 5.61 | 1.87 | 0.00 | 0.47 | 0.63 | 1.76 | 1.32 | 0.41 | 25 | | |
| LH117-226 | 226.0 | 2.11 | 0.07 | 5.69 | 0.91 | 15.95 | 28.48 | 0.18 | 0.08 | 0.01 | 7 | 1.4 | −9.3 |
| LH117-230 | 230.0 | 5.04 | 0.24 | 2.68 | 0.58 | 16.85 | 29.18 | 0.20 | 0.12 | 0.32 | 7 | 1.3 | −8.7 |

All oxides shown as percentages. Stable isotopes are shown as parts per million PDB. For drillhole locations see Fig. 1.

$\delta^{13}C_{carbonate}$ value for any one sample set by more than 1 standard deviation.

## RESULTS

### *The Thorntonia Limestone reference section*

The Thorntonia Limestone is well exposed in cliffs along the O'Shannassy River in the eastern Georgina Basin to the south of the Lawn Hill Structure (Fig. 4). For this study, we measured a well-exposed section through the basal part of the formation near Riversleigh Homestead [Universal Transverse Mercator Projection (UTM) Zone 54K, 0263752 7884580] (Table 1). The section was sampled every 1.5 m, and gamma readings were recorded every 50 cm (Fig. 4). The section represents the lower part of the basal depositional sequence of the Thorntonia Limestone and stops at the phosphatic hardground. The carbonate rocks are, for the most part, grainstone or less frequently wackestone with a large component of detrital echinoderm, trilobite, brachiopod, and other invertebrate skeletal material. Higher in the succession the rocks are phosphatic and locally glauconitic, and form a hardground similar to that encountered in the Lawn Hill Structure carbonate fill. The coarser carbonate sediments are commonly cross-bedded and contain large chert nodules in an interval 5 m above the base of the section.

Geochemically the Thorntonia Limestone is almost pure carbonate (silica content averages 1.1%) at the reference section site (Table 1). Gamma-log values decline upward away from bedrock as the detrital component declines and then increase rapidly near the phosphatized maximum flooding surface, probably because of an increase in K, U, and Th at the sea level high (Fig. 4). Predictably, the silica content is slightly greater near the basement and on the maximum flooding surface at the top of the measured section. The Mg/Ca ratio is relatively uniform throughout the section (mean 0.63 ± 0.02, $n = 14$), which suggests that dolomitization had reached equilibrium during diagenesis, an interpretation consistent with the high primary porosities in the fossiliferous coquina-like carbonate rocks. Isotopically, the carbonate rocks are relatively uniform, with $\delta^{13}C_{carbonate}$ values averaging 0.3 ± 0.7% ($n = 14$). Oxygen ($\delta^{18}O_{carbonate}$) values are similarly relatively uniform and lie close to the mean, −6.3 ± 0.9% ($n = 14$) (Fig. 4).

### *The carbonate ring*

Following a regional assessment, a section through the northern margin of the ring structure was selected for detailed sampling and analysis (Fig. 3 and Table 2). We assessed the facies, sampled the carbonate rocks, and took natural gamma-ray measurements on the outcrop at each of 22 localities across the carbonate and the Border Waterhole Formation.

The data show that, rather than the carbonates becoming younger toward the outer margins of the structure, as shown on existing map sheets

(Sweet and Hutton, 1982; Andrews, 1991), they simply fill a depression from either side. The facies succession changes inward to the center of the carbonate belt and then reverses. The facies zonation is somewhat condensed on the outside margin of the ring. Gamma logging shows increased counts on either margin of the outcrop belt (Fig. 3B). This suggests that the carbonates on either margin are higher in U, Th, and K, a finding that is consistent with increased clastic component, especially clays derived from bedrock.

Carbonates in the middle of the section (approximately LH6–LH16, Table 2 and Fig. 3) are dolomitic grainstones, much like those in the middle part of the Thorntonia Limestone reference section at Riversleigh (T6–T11, Table 1 and Fig. 4). Chert beds are sparse in these grainstones. Dolostones on the inner rim of the Lawn Hill Structure had precursor carbonates that were probably fine grained and included some disrupted chert beds. Fine-grained dolomudstones with disrupted chert beds were also found on the outer rim (LH17–LH22), much like those on the inner rim and similar to the dolomudstones at the base of the Riversleigh section (T0–T5). Polymict matrix-supported breccias occur on either side of the ring structure and are associated with increased gamma-ray counts.

Most of the samples from the ring structure are relatively pure carbonate with considerably less than 10% $SiO_2$ (Table 2 and Fig. 3E). The carbonates are dolomitized, much as in the reference section at Riversleigh Station, but the dolomitization has not proceeded to completion. Mg/Ca ratios average $0.47 \pm 0.15$, slightly lower than at Riversleigh. The clast-supported breccias (diamictites) on either side of the ring structure (samples LH03, LH04, LH17, and LH18, Table 2) have notably high silica content reflecting the inclusion of basement debris. In all cases Ni content is low.

The basal siliceous breccias beneath the Border Waterhole Formation were sampled at three localities and were found to be largely silica. In only one case, sample LH24, is there a significant carbonate content, and it has isotopically light carbon signatures (Table 2).

Stable isotope geochemistry of the samples from the section across the ring structure is very consistent (Fig. 3C and D). The $\delta^{13}C_{carbonate}$ values lie close to the mean at $0.6 \pm 1.3\%$, and those of $\delta^{18}O_{carbonate}$ with a mean of $-8.0 \pm 0.7\%$ (Table 3). The lower proportion of echinoderm debris in the carbonates from the ring structure, when compared with the Riversleigh reference section, may have led to the $\Delta^{13}C_{carbonate}$ values being slightly more positive, but statistically there is no difference. Only one sample, LH18, deviates significantly with a $\delta^{13}C_{carbonate}$ of $-4.7\%$. This sample lies close to the only mapped fault that crosses the section, which suggests the depleted isotopic value results from later fluid movement along the fault plane.

### *Carbonate breccia dikes*

Breccia dikes transecting basement rocks are common in drillcores from the Lawn Hill Structure. Following the examination of a large number of these cores, two were sampled from within the southwestern corner of the Lawn Hill Structure (cores LH116 and LH117). Sampling focused on the carbonate breccia dikes and the contact between the breccia and the bedrock (Table 3). The samples were collected in an attempt to determine the nature of carbonate breccia dikes. Were the dikes primary sediments (*i.e.*, contemporaneous with sedimentation) or the result of later diagenetic alteration? Or were they associated with the impact event forming the ring structure?

Major element geochemistry shows that all breccia dikes have a high carbonate content (approximately 30% CaO) and are comparable with breccias sampled from surface exposures across the ring structure (Table 3). In particular, Ni values are very low and comparable with carbonates from both the reference section at Riversleigh and the ring structure outcrops. Analyses at the contact between carbonate and shale at a depth of 214 m in core LH116 show the carbonate to be uncontaminated geochemically by contact with the floor of the ring structure. This implies that the carbonates were deposited into the ring structure rather than as part of the ring-forming process. The stable isotope signatures of the carbonate breccias from the core samples fit well within the normal range of values from the reference section and the outcrop samples from the ring structure (Table 3).

## DISCUSSION

### *Early Phanerozoic Earth*

The siliceous breccias at the base of the succession preserved in the inner margin of the carbonate ring of the Lawn Hill Structure are distinctive (Fig. 6A). Their texture is very similar to that generated in high-energy base-surge or fall-back deposits (*i.e.*, impact structure) on the lunar surface (see Lindsay, 1972a). The implication is that they are most likely fall-back breccias generated during impact. The rounding of grains results from clast interaction during high-velocity ejection in a gaseous cloud. The preservation of the basal breccia suggests that there was minimal time between the impact event and the filling of the crater by the carbonate succession. The light carbon isotopic value associated with the carbonate cement in the breccias suggests that it is a secondary cement, which is consistent with thin section observations. The isotopic values are also comparable with sample LH18 where fluid movement along the fault plane has modified the signature (Fig. 3C). The basal breccia (sample LH22) is low in Ni, which suggests little intermixing.

The carbonate breccia dikes that transect the basement rocks beneath the carbonate ring structure are somewhat enigmatic. The isotopic data suggest that the carbonate breccia dikes are normal carbonates generated in the platformal setting as part of the Thorntonia Limestone. If the dikes were formed by diagenetic processes, the isotopic signature would reflect the composition of the groundwater fluid passing through the sediments and become isotopically much depleted in $^{13}C$.

There are two obvious possibilities for the origin of the dikes: (1) They are injection dikes formed at the time of impact. (2) They are post-impact dike fillings or neptunian dikes. Injection dikes that involve similar lithologies have been described by Sturkell and Ormo (1997) in the Lockne impact structure in central Sweden. They described dikes and sills of a breccia surrounding large blocks in the crater similar to the Lawn Hill dikes. During hypervelocity impact, however, carbonates are superheated, disassociated, and dissolved in pore water within the bedrock before being driven as superheated solution ahead of the shock front and redeposited. Ultimately, the carbonates would have been injected at high pressure to form veins or dikes in the fractured rocks beneath the crater floor (Tingate *et al.*, 1996), a process that would have produced lighter isotopic values in the carbonates. Thus, if breccias were formed by impact or by later solution effects, the $\delta^{13}C_{carbonate}$ and $\delta^{18}O_{carbonate}$ values would be considerably lighter.

The other clue to their origin is the presence of the transgressive sandstone around the inner margin of the Lawn Hill ring structure. The transgressive sandstone overlies the basal siliceous breccia but lies beneath the Border Waterhole Formation. Further, the dikes are never seen in association with the transgressive sandstone but appear to be restricted to deeper sites within the crater. The low Ni values suggest that little, if any, meteoritic material has been included in the carbonates (assuming a nickel/iron bolide). This suggests that fractures on the crater floor were still open and free of sediment at the time of the transgression. The carbonate dikes are probably best described as neptunian dikes. They seem to have formed deeper in the impact structure independently of the basal siliceous breccias and the transgressive sandstone. The open fractures appear to have been deeper in the impact structure and were most likely filled by debris moving down slope from shallower carbonate platform settings on the crater rim. The impact thus occurred very shortly before or during the marine transgression, which indicates that the impact occurred at approximately 509–506 Ma. This is consistent with the fact that ejecta from the crater have not yet been encountered within the Thorntonia Limestone section to the south.

Facies analysis of the reference section indicates that the Thorntonia Limestone was deposited as a single depositional sequence representing one major sea level cycle. A slight depletion of the $\delta^{13}C_{carbonate}$ and $\delta^{18}O_{carbonate}$ values at approximately 9 m above basement suggests that the isotopic signature has been diagenetically modified by an increased flow of fluids through the system in the more open grainstone at that level. The increased abundance of echinoderm debris may also explain the slightly depleted $\delta^{13}C_{carbonate}$ and $\delta^{18}O_{carbonate}$ values at this level. Either way, the isotopic excursion is unlikely to be of global significance. In general, the stable isotopic compositions of the main body of carbonates from the ring structure at Lawn Hill are very similar to those of the Thorntonia Limestone reference section and fit well within the normal range expected from Lower/Middle Cambrian boundary carbonates (Brasier and Sukhov, 1998; Lindsay *et al.*, 2005). This, in combination with the fragmentary paleontological data, leaves little doubt that the structure was filled by marine carbonates during the Ordian and early Templetonian (early Middle Cambrian, 509–506 Ma).

At the crater margin, especially the inner margin of the ring structure, the Cambrian marine transgression is marked locally by a basal sandstone unit. Facies associations indicate a retrogradational phase of sedimentation (depositing a transgressive systems tract) as water depth increased. Above the transgressive sandstone, carbonate facies associations within the ring structure generally follow those of the Thorntonia Limestone and indicate deposition in a shallow marine subtidal to tidal setting. There are, however, some significant differences between the two settings. The succession at Lawn Hill is much thicker (by a factor of 4; Fig. 5), and it includes much more evidence of evaporitic facies in the section, especially the basal and middle section. The phosphatized hardgrounds in the crater fill and the Thorntonia section represent the maximum flooding surface, *i.e.*, the point where sedimentation rates slowed as water depth reached a maximum. Above the maximum flooding surface in the Thorntonia, deposition was progradational, which led to the formation of a shallowing upward succession (the highstand systems tract) that terminated at the top of the carbonate succession. In the crater fill, evaporitic facies decline rapidly above the maximum flooding surface in a response to rising sea level and a connection to basin-wide circulation.

The isotopic data from the Border Waterhole Formation are not significantly different from the main carbonate unit. The Border Waterhole Formation thus appears to be a facies variant of the basal part of the main carbonate unit with much of the breccia simply the result of dissolution of evaporitic facies. This is consistent with the observed lateral interfingering of the two units. The Border Waterhole Formation is most likely the collapsed remnant of a major evaporitic succession at the base of the carbonates, and grades laterally into the carbonates. It is the collapse of these basal evaporitic units that has caused the apparent chaotic nature of the bedding in the overlying carbonates within the crater. There is also evidence of increased slope failure during the early stages of deposition within the crater (polymict breccias with carbonate matrix) (Fig. 6B), which suggests that, in general, sediments were deposited on an unstable substrate with the inner slope being the more unstable, as might be expected in an impact-generated central uplift. The zones of instability coincide with increases in $SiO_2$ and $Al_2O_3$ content (Table 2 and Fig. 3E). This suggests that sediments began to fill the crater very shortly after the Lawn Hill Structure was formed, *i.e.*, before erosion had lowered the slope and removed unstable materials. The facies data also suggest that the slopes stabilized quickly, as there is a significant decline in evidence of slumping inward from the edges of the carbonate ring.

The Lawn Hill impact crater thus produced a major localized depression that formed a restricted evaporitic lagoonal environment in the early stages of the Middle Cambrian transgression. The sides of the crater were still covered by loose rubble that periodically collapsed and avalanched into the filling crater. With time the depression filled and sedimentation became less evaporitic and closer in depositional style to that of the Thorntonia Limestone.

The impact of the Lawn Hill bolide during the Early Phanerozoic thus created a distinctive microenvironment that, for a short time, enhanced local biospheric productivity. At least for a short period $E_h$ and pH may have been reduced because of restricted circulation, but carbonate deposition was maintained and ultimately enhanced across the crater. Throughout its life the restricted circulation within the structure resulted in a somewhat increased salinity apparently to the benefit of the local biosphere, certainly not to its detriment. Earth's biosphere at this time was at an important juncture as it headed into the Cambrian "explosion," which apparently was driven by an energetic and evolving Earth (Brasier and Lindsay, 2000; Lindsay and Brasier, 2002a,b).

### *Late Noachian Mars*

The surface environment of Late Noachian Mars was very different from that of Early Phanerozoic Earth. Morphological analysis of drainage basins suggests that, at best, water was never abundant on Mars. Precipitation was low, comparable to the Atacama Desert of Chile, one of the driest environments on Earth, and it was also sporadic (Stepinski and Stepinski, 2005). By Late Noachian, the water, a key element in the survival of any projected biosphere, was disappearing, and the internal energy of the planet was rapidly being exhausted. The results from the Mars Exploration Rover mission indicate a surface environment dominated by eolian processes but an environment in which water still played a significant role even if largely in the subsurface (Squyres and Knoll, 2005; Grotzinger *et al*., 2005; Knoll *et al*., 2005). Late Noachian sedimentary architecture appears to have been defined by the rise and fall of the water table beneath migrating dunes, an environment comparable with that of the present-day Antarctic Dry Valleys (Lindsay, 1972b) and many other desert environments.

While physical surface processes on Late Noachian Mars are comparable with terrestrial settings, the chemistry of the interstitial fluids can only be compared with extreme terrestrial environments. The sediments so far analyzed by the Mars Exploration Rover contain hematite and sulfates, in particular jarosite, which indicates deposition in a low pH environment (Grotzinger *et al*., 2005) comparable to the extreme environment of the Rio Tinto in Spain, where oxygenation, possibly biomediated, of a pyritic ore body releases groundwater charged with sulfuric acid and ferric iron into the river (Fernandez-Remolar *et al*., 2005). Carbonates, while present in martian meteorites, have not been identified on the martian surface. If the low pH environments identified by the Mars Exploration Rover are typical of Mars, sedimentary carbonates are unlikely to be abundant at the planet's surface.

If a surface-dwelling biota, perhaps dependent on solar radiation, ever developed early on the martian surface, it is only likely to have survived into the Late Noachian in suitable refuges where surface water was available. Moderate-sized impacts into the martian surface would excavate craters that penetrated the water table, releasing liquid water. As discussed, this water was likely to have been acidic and charged with sulfates. Loss of water to the atmosphere would have resulted in a further increase in total salinity, leading to a more extreme environment in biospheric terms. In spite of the extreme nature of the environment, experience on Earth shows that strongly acid environments can support a diverse community of microorganisms (Lopez-Archilla *et al*., 2001; Amaral Zettler *et al*., 2003; Baker and Banfield, 2003; Baker *et al*., 2004; Knoll *et al*., 2005). The main source of sediments accumulating in this setting would almost certainly have been eolian. In contrast to the Lawn Hill Crater, where the depositional architecture was defined by eustatic sea level change, the architecture of the martian crater fill was most likely determined by groundwater cycles, as was diagenesis of the accumulating sediments. The sporadic nature of precipitation on Mars implies that there would have been significant cycling of the water table.

A remaining issue is nutrient recycling in a closed depositional environment—especially the recycling of phosphorus and nitrogen. Experience in the Antarctic Dry Valleys suggests that eolian processes, while subtle, are an effective recycling mechanism in this extreme environment. Eolian sediment deposited on ice-covered lakes forms a dynamic equilibrium between downward movement, as a result of melting, during summer and upward movement of ice from ablation at the surface and freezing at the base. These eolian materials with their nutrients ultimately make their way to the lake floor probably though fractures in the ice (Priscu *et al*., 1998; Dore and Priscu, 2001). Since dust storms operate globally on Mars, they should be an effective mechanism for nutrient recycling in that setting as well. Thus small to medium impact structures may preserve the final record of any martian biosphere in a setting that could be explored relatively easily by shallow drilling.

## CONCLUSIONS

### *The Lawn Hill Structure*

1. Shatter cones, cone-in-cone structure, highly deformed suevites, and the broad uplift of basement rocks within the core of the ring structure provide strong evidence for an impact origin for the Lawn Hill Structure.
2. The texture of coarse clastic breccias at the base of the Border Waterhole Formation inside the carbonate ring is comparable texturally with lunar breccias, and these may be fall-back breccias formed during impact.
3. Facies and gamma-log patterns suggest that the carbonate ring structure was infilled symmetrically from both margins of the depositional trough.
4. Evidence of mass movement within the carbonates is consistent with the slopes of the depositional trough being unstable at the time of deposition, which suggests that the impact occurred shortly before the Middle Cambrian marine transgression and deposition of the Thorntonia Limestone.

5. Isotopically and geochemically, the carbonates sampled from the ring structure are identical to the Thorntonia Limestone from the Georgina Basin to the south and consistent with deposition in the Middle Cambrian. That is, the limestone and dolostone fill of the Lawn Hill Structure is an outlier of the Georgina Basin.
6. The carbonate breccia dikes transecting basement rocks are isotopically identical to other carbonates from the ring structure and the Thorntonia Limestone reference section. This, along with stratigraphic relationships, suggests that they are primary carbonate and, most probably, neptunian dikes. This implies that fractures in the base of the crater beneath the carbonates were open at the time of the Cambrian transgression and that the filling of the crater must have occurred very shortly after the impact structure formed.

On balance, the data suggest that the Lawn Hill Structure was formed shortly before or during the Middle Cambrian transgression at approximately 509–506 Ma, which left a deep crater with unstable walls and deep open fractures in the crater floor. The marine transgression quickly engulfed the site filling it with shallow water marine carbonates and evaporites. The depositional environment within the structure was more restricted than that encountered in the Thorntonia Limestone to the south. The structure initially formed an enclosed steep-sided lagoonal environment with deeper water but more saline conditions than elsewhere in the Georgina Basin. The crater was, however, regularly in contact with the global ocean. As the crater filled and sea level rose, its steep sides stabilized, and the depositional style settled in to one that was more consistent with the regional pattern of the Thorntonia Limestone. The net result is that the crater fill is more evaporitic in nature and four times the thickness of the nearby basinal succession.

The Lawn Hill Structure thus provided a protected microenvironment that, even though somewhat more evaporitic and saline than the surrounding basinal setting, followed the general depositional pattern of the nearby basin fill. The structure has survived as an erosional outlier and protected the stratigraphic record preserved within the crater.

*The martian analog*

Small to medium impact structures similar to the Lawn Hill Structure may well have provided biospheric refuges in the martian environment as the planet's water resources were depleted. There are numerous small to medium craters on the martian surface that have clearly defined flat floors, which suggests that they contain a sedimentary record. If so, they may preserve the best record of a late martian biosphere, if, indeed, a biosphere emerged on Mars and survived a sufficient amount of time. The recent discovery of small craters on Mars with ice ponded on their floors further supports the argument. These craters are likely to have penetrated the water table, thus providing a restricted aqueous environment in which life may have survived and been preserved as part of an eolian crater fill. The environment in these craters would have been extreme, but comparison with similar extreme settings on Earth suggests that a diverse ecology could be sustained. The intermittent nature of the precipitation on Mars suggests that the depositional architecture within the crater would have been controlled by groundwater cycles. Nutrient recycling could have been accomplished through eolian transport. Small to medium craters on Mars may thus be one of the best locations to core the sedimentary record in search for evidence of past life.

## ACKNOWLEDGMENTS

We thank Pasminco and Century Zinc mine site staff, especially Mark Saxon, for assistance in the field and Julie Cartlidge and Owen Green for laboratory support in Oxford. We also thank Allan Trieman and two anonymous reviewers for thoughtful reviews that significantly improved the paper. This research was conducted at the Lunar and Planetary Institute, which is operated by the Universities Space Research Association under contract CAN-NCC5-679 with NASA. This is LPI Contribution No. 1279.

## ABBREVIATIONS

Ga, billion years ago; Ma, million years ago; PDB, Vienna Pee Dee Belemnite; UTM, Universal Transverse Mercator Projection.

## REFERENCES


Amaral Zettler, L.A., Messerli, M.A., Laatsch, A.D., Smith, P.J.S., and Sogin, M.L, (2003) From genes to genomes: beyond biodiversity in Spain's Rio Tinto. *Biol. Bull*. 204, 205–209.

Ambrose, G.J., Kruse, P.D., and Putnam, P.E. (2001) Geology and hydrocarbon potential of the southern Georgina Basin, Australia. *Aust. Petrol. Product. Explor. Assoc. J*. 41, 139–163.

Andrews, S.J. (1991) *Surface Mapping of Cambrian Limestone at the Century Deposit North West Queensland, a Summary of Findings*, Report Number 17730, CRA Exploration Pty. Ltd., Melbourne, Australia.

Andrews, S.J. (1998) Stratigraphy and depositional setting of the upper McNamara Group, Lawn Hill Region, Northwest Queensland. *Econ. Geol*. 93, 1132–1152.

Baker, B.J. and Banfield, J.F. (2003) Microbial communities in acid mine drainage. *FEMS Microbiol. Ecol*. 44, 139–152.

Baker, B.J., Lutz, M.A., Dawson, S.C., Bond, P.L., and Banfield, J.F. (2004) Metabolically active eukaryotic communities in extremely acidic mine drainage. *Appl. Environ. Microbiol*. 70, 6264–6271.

Brasier, M.D. and Lindsay, J.F. (2000) Did supercontinent amalgamation trigger the 'Cambrian explosion'? In *Ecology of the Cambrian Radiation*, edited by R. Riding and A.Yu. Zhuravlev, Columbia University Press, New York, pp. 69–89.

Brasier, M.D. and Sukhov, S.S. (1998) The falling amplitude of carbon isotopic oscillations through the Lower to Middle Cambrian: northern Siberian data. *Can. J. Earth Sci*. 35, 353–373.

Brasier, M.D., Rozanov, A.Yu., Zhuravlev, A.Yu., Corfield, R.M., and Derry, L.A. (1994) A carbon isotope reference scale for the Lower Cambrian succession in Siberia: report of IGCP Project 303. *Geol. Mag*. 131, 767–783.

Brasier, M.D., Shields, G., Kuleshov, V.N., and Zhegallo, E.A. (1996) Integrated chemo- and biostratigraphic calibration of early animal evolution: Neoproterozoic to early Cambrian, southwest Mongolia. *Geol. Mag*. 133, 445–485.

Carter, E.K. and Öpik, A.A. (1961) *Lawn Hill 4-Mile Geological Map Sheet Series, Explanatory Notes SE/54-9*, Bureau of Mineral Resources, Geology and Geophysics, Canberra, Australia.

Chamberlain, A.K. (1984) Surface gamma-ray logs: a correlation tool for frontier areas. *Am. Assoc. Petrol. Geol. Bull*. 68, 1040–1043.

de Keyser, F. (1969) The phosphate-bearing Cambrian formations in the Lawn Hill and Lady Annie districts, northwestern Queensland. In *Bureau of Mineral Resources, Geology and Geophysics, Australia, Record, Vol. 147*, Bureau of Mineral Resources, Geology and Geophysics, Canberra, Australia.

Dore, J.E. and Priscu, J.C. (2001) Phytoplankton phosphorus deficiency and alkaline phosphatase activity in the McMurdo Dry Valley lakes, Antarctica. *Limnol. Oceanogr*. 46, 1331–1346.

Fernandez-Remolar, D.C., Morris, R.V., Gruener, J.E., Amils, R., and Knoll, A.H. (2005) The Rio Tinto Basin, Spain: mineralogy, sedimentary geobiology, and implications for the interpretation of outcrop rocks at Meridiani Planum, Mars. *Earth Planet. Sci. Lett*. 240, 149–167.

Grotzinger, J.P., Arvidson, R.E., Bell, J.F., III, Calvin, W., Clark, B.C., Fike, D.A., Golombek, M., Greeley, R., Haldemann, A., Herkenhoff, K.E., Jolliff, B.L., Knoll, A.H., Malin, M., McLennan, S.M., Parker, T., Soderblom, L., Sohl-Dickstein, J.N., Squyres, S.W., Tosca, S.W., and Watters, W.A. (2005) Stratigraphy and sedimentology of a dry to wet eolian depositional system, Burns formation, Meridiani Planum, Mars. *Earth Planet. Sci. Lett*. 240, 11–72.

Hutton, L.J. (1992) *Report on Investigation of Postulated Astrobleme, Lawn Hill. Report to the Australian Heritage Commission*, Australian Heritage Commission, Canberra.

Knoll, A.H., Carr, M., Clark, B., Des Marais, D.J., Farmer, J.D., Fischer, W.W., Grotzinger, J.P., McLennan, S.M., Malin, M., Schroder, C., Squyres, S., Tosca, N.J., and Wdowiak, T. (2005) An astrobiological perspective on Meridiani Planum. *Earth Planet. Sci. Lett*. 240, 179–189.

Lindsay, J.F. (1972a) Sedimentology of clastic rocks from the Fra Mauro region of the Moon. *J. Sediment. Petrol*. 42, 19–32.

Lindsay, J.F. (1972b) Barchan dunes in lower Victoria Valley, Antarctica. *GSA Bull*. 84, 1799–1806.

Lindsay, J.F. and Brasier, M.D. (2002a) Did global tectonics drive early biosphere evolution? Carbon isotope record from 2.6 to 1.9 Ga carbonates of Western Australian basins. *Precambrian Res*. 114, 1–34.

Lindsay, J.F. and Brasier, M.D. (2002b) A comment on tectonics and the future of terrestrial life—reply. *Precambrian Res*. 118, 293–295.

Lindsay, J.F. and Korsch, R.J. (1989) Interplay of tectonics and sea-level changes in basin evolution: an example from the intracratonic Amadeus Basin, central Australia. *Basin Res*. 2, 3–25.

Lindsay, J.F., and Leven, J.F. (1996) Evolution of a Neoproterozoic to Palaeozoic intracratonic setting, Officer Basin, South Australia. *Basin Res*. 8, 403–424.

Lindsay, J.F., Korsch, R.J., and Wilford, J.R. (1987) Timing the breakup of a Proterozoic supercontinent: evidence from Australian intracratonic basins. *Geology* 15, 1061–1064.

Lindsay, J.F., Kruse, P.D., Green, O.R., Hawkins, E., Brasier, M.D., Cartlidge, J., and Corfield, R.M. (2005) The Neoproterozoic-Cambrian record in Australia: a stable isotope study. *Precambrian Res*. 142, 113–133.

Lopez-Archilla, A.L., Marin, I., and Amils, R. (2001) Microbial community composition and ecology of an acidic aquatic environment: the Tinto River, Spain. *Microb. Ecol*. 41, 20–35.

Öpik, A.A. (1956) Cambrian geology of Queensland. In *Bureau of Mineral Resources Geology and Geophysics, Australia, Bulletin, Vol. 49*, Bureau of Mineral Resources, Geology and Geophysics, Canberra, Australia, pp. 25–54.

Page, R.W., Jackson, M.J., and Krassay, A.A. (2000) Constraining sequence stratigraphy in northern Australian basins: SHRIMP U-Pb zircon geochronology between Mt Isa and McArthur River. *Aust. J. Earth Sci.* 47, 431–459.

Priscu, J.C., Fritsen, C.H., Adams, E.E., Giovanni, S.J., Paerl, H.W., McKay, C.P., Doran, P.T., Gordon, D.A., Lanolil, B.D., and Pinckney, J.L. (1998) Perennial Antarctic lake ice: an oasis for life in a polar desert. *Science* 280, 2095–2098.

Shoemaker, E.M. and Shoemaker, C.S. (1996) The Proterozoic impact record of Australia. *Aust. Geol. Survey Org. J. Geol. Geophys*. 16, 379–398.

Southgate, P.N. (1988) A model for the development of phosphatic and calcareous lithofacies in the Middle Cambrian Thorntonia Limestone, northern Georgina Basin, Australia. *Aust. J. Earth Sci*. 35, 111–130.

Squyres, S.W. and Knoll, A.H. (2005) Sedimentary rocks at Meridiani Planum: origin, diagenesis, and implications for life on Mars. *Earth Planet. Sci. Lett*. 240, 1–10.

Stepinski, T.F. and Stepinski, A.P. (2005) Morphology of drainage basins as an indicator of climate on early Mars. *J. Geophys. Res*. 110(E12S12), 1–7.

Stewart, A.J. and Mitchell, K. (1987) Shatter cones at the Lawn Hill circular structure, northwest Queensland: presumed astrobleme. *Aust. J. Earth Sci*. 34, 477–485.

Sturkell, E.F.F. and Ormo, J. (1997) Impact-related clastic injections in the marine Ordovician Lockne impact structure, central Sweden. *Sedimentology* 44, 793–804.

Sweet, I.P. and Hutton, L.J. (1982) *Lawn Hill Region, Queensland, 1:100,000 Geological Map Commentary*, Bureau of Mineral Resources, Geology and Geophysics, Canberra, Australia.

Szulc, S.A. (1992) The stratigraphic reconstruction of a mega-breccia; a sedimentological study of the south western corner of the Lawn Hill Outlier [Honours Thesis], James Cook University, Townsville, Australia.

Tingate, P.R., Lindsay, J.F., and Marshallsea, S.J. (1996) Impact structures as potential petroleum targets: Gosses Bluff, a Late Jurassic examples in Central Australia. *Aust. Geol. Survey Org. J. Aust. Geol. Geophys*. 16, 529–552.

Wilson, I.H. and Hutton, L.J. (1980) Geological field work in Mount Isa district—August and September, 1980. *Geol. Survey Queensland Record* 34, 12–18.

Address reprint requests to:
*John Lindsay*
*Lunar and Planetary Institute*
*3600 Bay Area Boulevard*
*Houston, TX 77598*

*E-mail:* Lindsay@lpi.usra.edu

**This article has been cited by:**

1. Penny A. Morris . 2008. Tribute to John F. LindsayTribute to John F. Lindsay. *Astrobiology* **8**:4, 707-713. [Citation] [PDF] [PDF Plus]